American Mineralogist, Volume 84, pages 746–753, 1999

Reconnaissance fluid inclusion study of the Morefield pegmatite, Amelia County, Virginia

JOHN R. SMEREKANICZ* AND FRANCIS Ö. DUDÁS†

Geological Sciences Program, Old Dominion University, Norfolk, Virginia 23529, U.S.A.

ABSTRACT

Over 90% of the fluid inclusions in quartz, topaz, and beryl from the Morefield pegmatite, Amelia Co., Virginia, contain mixed CO_2-H_2O fluids. In order of abundance, there are four inclusion types: (1) three-phase, l-l-v; (2) two-phase, H_2O-rich; (3) three- or four-phase, l-v-s and l-l-v-s; and (4) two-phase, CO_2-rich. CO_2-rich inclusions formed by necking of inclusions containing mixed fluids. Topaz and quartz contain all four inclusion types, and all types occur throughout the pegmatite, although no H_2O-rich inclusions occur in beryl. Quartz from gneiss that hosts the pegmatite contains dominantly H_2O-rich inclusions. Most inclusions are secondary and occur along healed fractures. Possible primary inclusions occur only among those that contain solids. All inclusions homogenize into the liquid phase; a few homogenize to liquid CO_2. H_2O-rich inclusions with <2 wt% NaCl (eq.) and homogenization temperatures <200 °C occur in the host gneiss and throughout the pegmatite and are interpreted to contain meteoric waters. H_2O-rich and mixed fluid inclusions with 3–7 wt% NaCl (eq.) and homogenization temperatures >290 °C contain fluids interpreted to derive primarily from the pegmatite. Inclusions with salinities between 3–13 wt% NaCl (eq.) and intermediate homogenization temperatures are in part cooled equivalents of the pegmatite fluids, but the origin of those with salinity >7 wt% NaCl (eq.) is uncertain. Homogenization temperatures for CO_2 indicate average CO_2 densities near 0.65 g/cm^3. For mixed fluids homogenizing near 300 °C and this CO_2 density, the trapping pressure is estimated to be 2.5 kb. Neither age relations nor physical proximity tie the Morefield pegmatite to known granitic intrusions. Fluid compositions preclude a genetic relation between the pegmatite and its host gneisses.

INTRODUCTION

Granitic pegmatites potentially record the history of late magmatic fluids, and complex pegmatites can offer insight into the geochemical transport both of “immobile” (Nb, Ta) and volatile (F, Cl, B) components. Tracing the evolution of fluids in pegmatites therefore has been a significant focus of research. The goals of this reconnaissance study of fluid inclusions in a complex, rare-element pegmatite were to determine how much of the fluid history was preserved, to estimate the conditions under which fluids were trapped, and to constrain the minimum conditions of pegmatite formation.

Among the pegmatites in central Virginia, Morefield is the only one that is actively mined (Sweet and Penick 1986). This study focused on Morefield because outstanding exposure of the pegmatite offered unique sampling control, and prior work provided a good geological foundation (Brown 1962; Geehan 1953; Jahns et al. 1952; Lemke et al. 1952). At the same time, most work on pegmatites in this area concerned their mineralogy (Glass 1935; Kearns 1992a, 1992b, 1993a, 1993b; Mitchell and McGavock 1960; Sinkankas 1968; Smerekanicz et al. 1991), whereas our emphasis is on petrogenesis. Accordingly, we attempt to describe the evolution of fluids associated with the pegmatite.

Inclusions in pegmatites are varied, but commonly contain CO_2-rich and mixed CO_2-H_2O fluids. Studies of other pegmatites indicate that few inclusions are trapped at the magmatic stage (Cook 1979; London, 1985; Roedder 1984; Thomas and Spooner 1988a, 1988b, 1992; Weis 1953; Williams and Taylor 1996), and that most inclusions represent late-stage hydrothermal fluids (London 1986). Those inclusions interpreted to be associated with magmatic conditions can have high salinities, and they commonly also contain various solid phases, including oxides, fluorides, chlorides, and borates in addition to topaz and micas (Foord et al. 1991).

GEOLOGICAL SETTING

The pegmatites of Amelia County, Virginia (Fig. 1), are small, tabular bodies that crosscut the prevailing foliation of the enclosing, amphibolite-grade gneisses (Brown 1962). There are no detailed geologic maps of the area: There is virtually no outcrop, and up to 20 m of saprolite cover bedrock. The Morefield pegmatite intrudes rocks assigned to the Maidens Gneiss (Farrar 1984). These hornblende, biotite, and porphyroblastic biotite-garnet gneisses are part of the Goochland terrane, which is defined by the extent of Grenville-aged granulite-grade rocks within the Piedmont (Farrar 1984; Glover et al. 1982; Rankin et al. 1989). Retrograde metamorphism under amphibolite-grade conditions occurred during the Paleozoic; hornblende and biotite in the gneiss have $^{40}Ar/^{39}Ar$ cooling ages between 280 and 260 Ma (Durrant et al. 1980).

---

*Present address: Golder Associates, Mt. Laurel, New Jersey 08054, U.S.A.

†Present address: Tark Geosciences, Massachusetts 01821, U.S.A. E-mail: fold@norfolk.infi.net

0003-004X/99/0506–0746$05.00

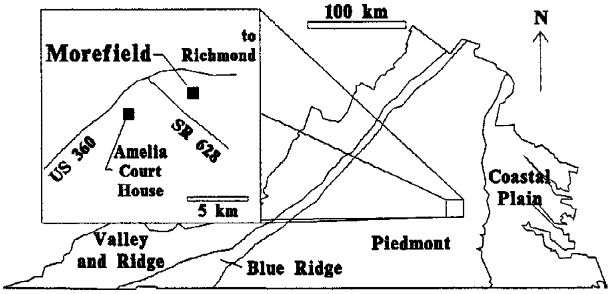

FIGURE 1. Physiographic province map of Virginia, showing location of the Morefield pegmatite.

TABLE 1. Minerals reported from the Morefield pegmatite*

Sulfides	**Oxides and Hydroxides**	**Halides**
chalcopyrite	cassiterite	chiolite
galena	columbite-tantalite	cryolite
pyrite	ilmenite	elpasolite
	manganotantalite	fluorite
Phosphates	microlite	pachnolite
fluorapatite	pyrolusite	prosopite
monazite	rutile	ralstonite
pyromorphite	samarskite	thomsenolite
strengite	strüverite	
triplite		
Nesosilicates	**Phyllosilicates**	**Tectosilicates**
garnet: spessartine	biotite	albite
phenakite	cookeite	anorthoclase
topaz	kaolinite	microcline
zircon	muscovite	oligoclase
	zinnwaldite	orthoclase
		quartz
Sorosilicates	**Cyclosilicates**	
allanite	beryl	
bertrandite	tourmaline	

*Modified from Dietrich (1990) and Kearns (1993).

The Morefield pegmatite, discovered in 1929, is at least 360 m long (possibly up to 670 m; Kearns 1993b), up to 10 m wide, and is oriented 047°/80° NW (Brown 1962; Lemke et al. 1952). It is cut almost perpendicularly by at least three diabase dikes. Morefield is a complex pegmatite (Fig. 2) that was investigated as a possible source of Nb and Ta (Geehan 1953), and produced mica, feldspar, columbite-tantalite, and gem beryl and topaz (Sweet and Penick 1986). In 1948, the US Bureau of Mines bulldozed five exploration trenches across the strike of the pegmatite, drilled five inclined core holes to a maximum vertical depth of 65 m, and extended underground workings to a depth of almost 40 m (Geehan 1953). Since the mine reopened in 1986, there has been development on the 20 m (60 foot) level of the mine (referred to as the 45 foot level in prior literature; Kearns 1993b), and a second shaft has been sunk to the northeast along the strike of the pegmatite.

The southwestern end of Morefield is a simple pegmatite. Northeastward, the complex part of the pegmatite extends about 150 m. Four zones are present: a thin, discontinuous border zone at the contact with host gneisses; a peripheral or wall zone consisting of coarse- to medium-grained, albite-rich rock; an intermediate zone containing large crystals of quartz, amazonite, topaz, and mica embedded in albite (cleavelandite); and a core zone consisting of almost pure, coarse smoky quartz. Several unusual minerals occur at Morefield (Table 1), the most interesting of which are secondary alumino-fluorides (Kearns 1993a, 1993b) and phosphates (Kearns 1992a; Smerekanicz et al. 1991). In the intermediate zone, crystals of amazonite and white topaz commonly exceed 50 cm, whereas columbite-tantalite and spessartine occur scattered throughout the peripheral and intermediate zones. Beryl occurred in the upper portion of the pegmatite that was removed by surface mining. Prospects for recovering gem-quality topaz, beryl, and garnet at Morefield are limited by pervasive fracturing. Throughout the intermediate and core zones, fractures are spaced approximately <5 cm apart, and coherent pieces larger than about 5 cm are rare.

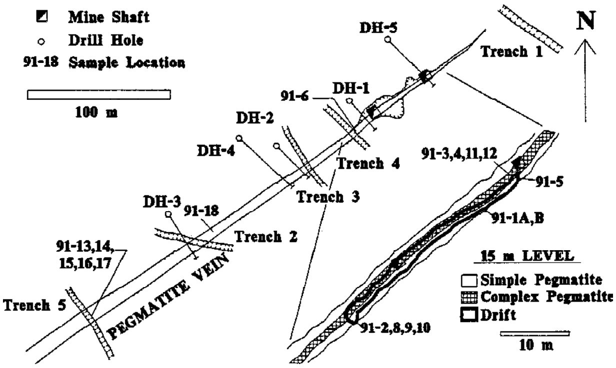

FIGURE 2. Surface and 15 m level maps of Morefield, showing trench, drill hole, and sample locations.

The Amelia pegmatites have been dated using K-Ar and Rb-Sr methods. Mica and albite samples gave K-Ar ages between 212 ± 6 and 416 ± 21 Ma, and contained excess argon (Laughlin 1966, 1968, 1969); the best K-Ar estimate is 248 ± 4 Ma, based on three muscovite samples. Rb-Sr analyses on micas gave ages of 261 ± 13 and 280 ± 14 Ma (Deuser and Herzog 1962), but are also suspect because of open-system behavior. The pegmatite predates ca. 200 Ma diabase dikes (Dunning and Hodych 1990) that intruded during Mesozoic extension and opening of the Atlantic Ocean, and the young K-Ar dates could reflect resetting of micas during diabase intrusion. If the ca. 250 Ma estimate is correct, the Amelia pegmatites are significantly younger than the Acadian pegmatites of North Carolina (Kings Mountain: 340–350 Ma; Kish 1977; Spruce Pine: 390–395 Ma, Goldberg et al. 1992) and the Pennsylvanian age suggested by Jahns et al. (1952). They are also younger than the most likely candidate for a parental granitic magma source, the Petersburg Granite (330 ± 8 Ma by U-Pb on zircon; Wright et al. 1975).

Morefield is about 25 km from the Petersburg Granite, the nearest exposed Paleozoic intrusive, and is separated from it by the Hylas mylonite zone (which may be coeval with the granite) and the Triassic Richmond Basin. The muscovite K-Ar age for Morefield is consistent with Alleghanian cooling ages in hornblende and biotite from the enclosing gneiss (Durrant et al. 1980). Alleghanian, primarily S-type granite plutons as young as 265 Ma are present in the southern Appalachians (Fullagar 1971; Fullagar and Butler 1979), but none are near the Amelia pegmatites. Neither age relations nor physical proximity links the pegmatites to known granitic intrusions.

SAMPLING METHODS

Twenty-one samples were taken from the pegmatite and its host rocks (Fig. 2). We sampled the peripheral (outer) and intermediate and core (inner) zones of the pegmatite, and collected quartz from a foliation-parallel segregation in the host gneiss. Thin sections were prepared of 15 samples (7 quartz, 5 quartz with albite, 2 topaz, and 1 beryl). Spessartine chips examined in immersion oil contained no fluid inclusions and were too thoroughly fractured to be used for fluid inclusion study. Nine samples were used for thermometry (Table 2). We collected microthermometric data on 3 to 6 chips of each selected sample, using a Fluid Inc. gas-flow stage. Synthetic fluid inclusions in quartz (prepared by SynFlinc) were used as calibration standards. Measurements were made of six phase transitions: the melting points of solid CO_2 (Tm CO_2), ice (Tm H_2O), and CO_2 clathrate hydrate (Tm CO_2hyd), and the homogenizations of CO_2 liquid and vapor (Th CO_2), H_2O liquid and vapor (Th H_2O), and H_2O liquid with CO_2 liquid (Th CO_2-H_2O). Replicate temperature determinations on calibration standards and samples indicate precision of 0.1 °C on measurements of Tm CO_2, Tm H_2O and Th CO_2, 1 °C on measurements of Th H_2O and Th CO_2-H_2O, and ~0.5 °C on measurements of Tm CO_2hyd. Fluid inclusion data were processed using FLINCOR (Brown 1989). Salinities were calculated using the revised equations in Bodnar (1993) for NaCl-H_2O and Darling (1991) for H_2O-NaCl-CO_2.

RESULTS

Description of fluid inclusion types

Four fluid inclusion types can be distinguished. Two are end-members: H_2O-rich inclusions that show no evidence of CO_2, and CO_2 inclusions that show no evidence of H_2O. A mixture of CO_2 and H_2O occurs in a third type, and the fourth type contains solids in addition to two or three fluid phases. Essentially all inclusions are secondary or pseudosecondary, occurring along healed fractures. A few isolated inclusions are not associated with microfractures and could be primary; these invariably contain solid phases.

Water-rich inclusions contain two fluid phases at room temperature, with the liquid phase usually exceeding 90% by volume. Many of these inclusions have negative crystal shapes, and are smaller than 20 µm. These usually comprise <10% of the inclusion population; they are absent from 91-20, the beryl sample, and represent >95% of the inclusions in 91-19, the country rock quartz sample.

Inclusions that contain almost pure CO_2 are relatively rare and, because they occur in association with mixed CO_2-H_2O inclusions along healed microfractures, probably result from necking down of inclusions that contained mixed fluids. CO_2-rich inclusions are 10–25 µm in diameter, and usually exhibit negative crystal shapes.

About 90% of all inclusions contain mixed fluids. CO_2:H_2O ranges from 25:75 to 100:0, but is most commonly between 25:75 and 50:50 (apparent volumes at room temperature). Inclusions with mixed fluids average 10–40 µm in diameter, and show various morphologies, from mature, negative crystals with CO_2 contents consistently >90 vol%, to irregular, amoeboid shapes. The largest inclusions are up to 300 µm in diameter, are planar and irregular, invariably contain inconsistent phase ratios, and have CO_2 contents near 90 vol%.

Inclusions that contain solid phases represent less than two percent of the inclusion population, and occur only in samples from the inner zone of the pegmatite. They contain three (l-v-s) or four (l-l-v-s) phases. Most of these inclusions are irregular, with diameters between 25–50 µm. As many as five solids occur in individual inclusions, and include opaque and transparent, and both isotropic and anisotropic minerals. Isotropic phases did not dissolve during heating, and we have no evidence for the presence of halite or sylvite. Anisotropic minerals have varying habits and relief, and some show parallel extinction. Though this group includes the only possibly primary inclusions (isolated inclusions not occurring along microfractures), we found no solid-

TABLE 2. Sampling and distribution of thermometric observations

Samples	Mineral	No. of Incls	Tm CO_2	Th CO_2	Tm CO_2-hyd	Tm H_2O	Th H_2O	Th CO_2-H_2O
				Inner Zone				
91-4	quartz	45	22	16		17	20	
91-9	quartz	64	47	44	20	17	16	13
91-11	topaz	49	24	14	24	4	18	28
91-20	beryl	45	45	42	21			18
Total		203	138	116	65	38	54	59
				Outer Zone				
91-5	quartz	41	25	12	13		6	4
91-8	quartz	45	21	18		22	18	
91-10	quartz	96	78	70	14	17	12	12
91-15	quartz	36	15	15	11	17	20	3
Total		218	139	115	38	56	56	19
				Host Gneiss				
91-19	quartz	10				10	5	
Totals		431	277	231	103	104	115	78

bearing inclusions appropriate for thermometry: Their phase ratios are inconsistent, both in fluid composition and in number and volume of solid phases, and most also show evidence of stretching, necking, or leakage.

Melting of solid CO_2: The purity of CO_2

Melting temperatures for solid CO_2 range from –56.3 to –57.4°C. Observations above the melting temperature of pure CO_2 (–56.6 °C), result from an unresolved error in stage calibration, affecting all observations on single chips of topaz and beryl; other chips from these samples yield results comparable to those determined on quartz. In the outer zone of the pegmatite, 139 measurements of Tm CO_2 average –56.8(0.2) °C; in the inner zone, 138 observations average –56.7(0.2) °C. The CO_2 phase in the different zones and along the sampled length of the pegmatite is homogeneous. The lowest observed melting temperature, –57.4 °C, indicates that the amount of CH_4 or similar components is less than <5 mol%.

Melting of ice and CO_2 clathrate hydrate: Salinity of aqueous fluids

Ice-melting temperatures, measured only in H_2O-rich inclusions, range down to –9.0 °C. Three temperature ranges, representing different salinities, occur in the samples (Fig. 3). Inclusions in inner zone quartz (sample 91-4) have Tm H_2O between –5 and –9°C, and NaCl equivalent [(wt% NaCl (eq.)] salinity >5 wt%. The most abundant inclusions in both inner and outer zone samples have Tm H_2O between –4 and –5°C, and salinity between 3 and 6 wt% NaCl (eq.). Samples from both zones, and from the host gneiss, have inclusions with Tm H_20 between –1.2 and 0 °C, indicating salinity <2 wt% NaCl (eq.). These distinct inclusion populations occur along individual healed fractures, though single samples contain inclusions from two or all three groups. The calculated maximum salinity of H_2O-rich fluids is 13 wt% NaCl (eq.).

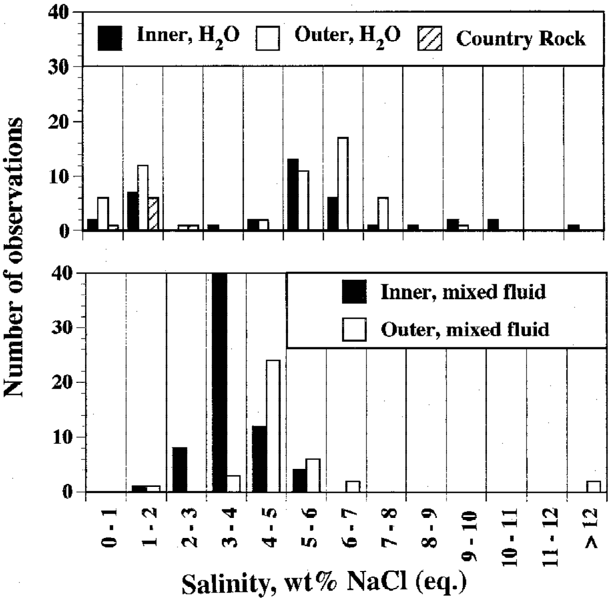

FIGURE 3. Salinity histograms for H_2O-rich **(top)** and mixed fluid **(bottom)** inclusions.

Salinity of inclusions containing mixed fluids was estimated from the dissociation temperature of CO_2 clathrate hydrate, which ranges between 2.0 and 9.2 °C. Salinities range from 1.6 to 13 wt% NaCl (eq.). Uncertainty in the temperature determinations results in some spread in the data, and statistically, no difference exists between observations on inner zone and outer zone samples. Inner zone samples have an average clathrate melt temperature of 8.2(0.4) °C, which translates into a salinity of 3.7(0.8) wt% NaCl (eq.). Outer zone samples have an average clathrate melt temperature of 7.3(1.3) °C, providing a salinity estimate of 5.1(2.0) wt% NaCl (eq.). Salinity values derived from ice-melting and clathrate-melting temperatures are internally consistent, although salinities derived from clathrate melting temperatures are somewhat lower. Most inclusion fluids are relatively dilute, containing only 3–7 wt% NaCl (eq.).

Homogenization of CO_2: Density of CO_2

In all inclusions that contain both liquid and vapor CO_2 at room temperature, CO_2 homogenizes into the liquid phase. Homogenization temperature ranges between 16 and 31 °C (type I inclusions of Rosso and Bodnar 1995), with only 4 of 231 measurements below 23 °C. There is no statistical difference between average values for inner [29.2(2.2) °C, n = 116] and outer zone [28.0(1.8) °C, n = 115] samples but, in the outer zone samples, some microfractures contain inclusions with Th CO_2 systematically between 26–27 °C. Computed CO_2 densities for the average Th CO_2 of inner and outer zone samples are 0.63 and 0.66 g/cm^3, respectively. The minimum density, 0.51 g/cm^3, occurs in inclusions in the inner zone, whereas the maximum density, 0.81 g/cm^3, occurs in inclusions from the outer zone.

Homogenization of H_2O and CO_2-H_2O: Density of aqueous and mixed fluids

In H_2O-rich inclusions, homogenization is always into the liquid phase, and occurs between 130 and 340 °C, with a single outlying measurement at 380 °C (Fig. 4). In inclusions of the inner zone, there are two populations: one homogenizes at temperatures above 280 °C, whereas the other homogenizes between 130 and 230 °C. There are no measurements between 230 and 280 °C. Inclusions in the outer zone show a broad distribution, and no homogenization temperatures >290 °C.

At temperatures >31 °C, inclusions containing mixed fluids consist of liquid H_2O and liquid CO_2, and 70 of 78 of these inclusions homogenize into the aqueous phase at temperatures between 280 and 360 °C. In the inner zone, 57 of 59 measurements yield an average temperature of 310(12) °C. The other two inclusions homogenize near 240 °C. The average homogenization temperature for 12 outer zone inclusions, 316(9) °C (excluding one observation at 360 °C), is indistinguishable from that of inner zone samples. Six inclusions in one microfracture in 91-10 (outer zone) homogenize into the CO_2 phase, and the average homogenization temperature for this population is 250 °C. This CO_2-rich inclusion population is absent from inner zone samples.

Inclusions with mixed and H_2O-rich fluids occur in quartz lenses in the host gneiss (sample 91-19), but about 95% of these are H_2O-rich. In this sample, only H_2O-rich inclusions are appropriate for thermometry; those with mixed fluids show inconsistent phase ratios, and are generally <5 µm in diameter.

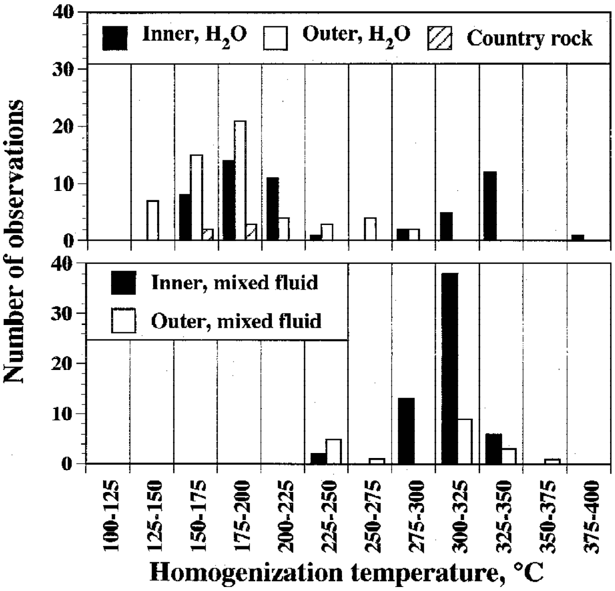

FIGURE 4. Histograms of homogenization temperatures for H_2O-rich (top) and mixed fluid (bottom) inclusions.

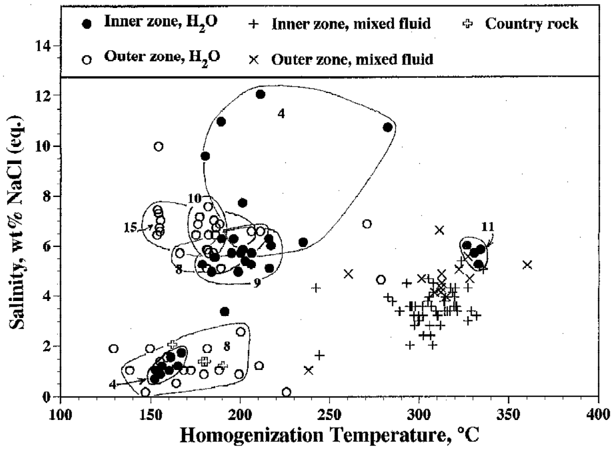

FIGURE 5. Combined plot of salinity and homogenization temperatures shows clusters of fluids rather than continuous trends of compositional change.

Water-rich inclusions in 91-19 have low Th H_2O (150–180°C) and low salinities [<1.5 wt% NaCl (eq.)].

Fluid densities for H_2O-rich inclusions (Zhang and Frantz 1987) range from a minimum of 0.73 g/cm^3 for inclusions in topaz from the inner zone, to a maximum of 0.98 g/cm^3. The minimum density for inclusions in quartz is 0.81 g/cm^3. Most inclusions in the pegmatite have densities between 0.8–0.9 g/cm^3, whereas inclusions in the host gneiss have densities > 0.9 g/cm^3.

Combining calculated salinity and observed homogenization temperatures (Fig. 5) reinforces our interpretation that inclusions at Morefield were trapped from discrete pulses of fluid traveling along microfractures during cooling of the pegmatite. In the inner zone samples, four such fluid pulses can be distinguished, varying in salinity and homogenization temperature. Although the homogenization temperatures, alone, suggest a continuous range of conditions between 130 to 250 °C, the combination of data shows discrete fluid pulses.

DISCUSSION

Conditions of fluid trapping

To interpret conditions of fluid trapping, some selection of data is required. Of particular interest are the data from topaz and beryl: These minerals allow some insight into how conditions in the complex, inner part of the pegmatite might differ from those in the outer zone, the simple pegmatite. Water-rich inclusions are absent from the beryl sample: Mixed fluids with trapping temperatures >330 °C are the earliest fluids preserved in the pegmatite and are implicated in the formation of the complex pegmatite. Water-rich and mixed fluids are present in topaz and quartz, and occur in both inner and outer zone samples. In topaz, some inclusions with water-rich fluids homogenize in approximately the same temperature range (290–330 °C) as inclusions with mixed fluids. Although these observations suggest that a mixed fluid underwent immiscible separation into two compositionally distinct fluids, fluid compositions are not compatible with solvi in the CO_2-H_2O-NaCl system: Both water-rich and mixed fluids are on the water-rich side of the solvus, and the CO_2-rich fluid, which should have over 70 vol% CO_2 at 25 °C, is not represented in the inclusions found in topaz. We have no observational evidence of immiscibility, i.e., we have not seen water-rich and CO_2-rich fluids coexisting along single microfractures, except where we also suspect necking or inclusion leakage. What appear to be two different fluids in topaz probably represent fluids with variable CO_2 content, although in some inclusion CO_2 is not detectable optically.

The best constraint on the conditions of trapping, in the absence of independent estimators of temperature or pressure (mineral or isotopic geothermometers or geobarometers), comes from experiments on the CO_2-H_2O-NaCl system. In salt-free systems, water-rich fluids (<20 vol% CO_2 at 25 °C) are immiscible with CO_2-rich fluids (>70 vol% CO_2 at 25 °C) at ~300 °C and 500 bars pressure (Sterner and Bodnar 1991). At lower temperatures, the solvus widens, with a greater compositional contrast between the coexisting fluids. The minimum pressure of trapping, 0.5 kb, can be inferred from the solvus in the salt-free system.

Experimental data are scarce for salt-bearing systems at temperatures below 500 °C. The data of Frantz et al. (1992) indicate that, at 500 °C, all fluids containing approximately <30 wt% CO_2 remain in the one-fluid field. As salinity decreases, the amount of CO_2 required for immiscibility increases. For fluids with salinity between 3–6 wt% NaCl (eq.), unmixing would occur at 500 °C and 2 kb only if their CO_2 content exceeded ~45 wt%: At Morefield, none of the inclusions with mixed fluids are this rich in CO_2. At 300 °C, lower CO_2 content is required for immiscibility, and unmixing could occur during cooling. The bulk of the mixed fluids in the inclusions represent fluids along the water-rich limb of the CO_2-H_2O solvus. Only in 91-10, in the outer zone, are there six inclusions that homogenize to CO_2; these may represent fluids from the CO_2-

rich side of the solvus. These inclusions homogenize at 240 °C, and are not cognate with the mixed, 300 °C fluid. These observations suggest that most inclusions trapped a homogeneous fluid at approximately >300 °C, and that, if unmixing of CO_2 and H_2O occurred during cooling, it occurred <250 °C. In the samples we examined, we have no evidence of unmixing at higher temperature.

The computed location of the water-rich solvus in the CO_2-H_2O-NaCl system at lower temperatures (Fig. 6; Brown and Lamb 1989), though poorly constrained by experiment, suggests that trapping pressure was probably around 2.5 kb. This estimate is based on the range of CO_2-H_2O homogenization temperatures (290–330 °C) and the density of the CO_2 phase (~0.65 g/cm^3), determined from the CO_2 liquid-vapor homogenization temperature. Homogenization of H_2O-rich inclusions near 300 °C indicates trapping temperatures as high as 500 °C, if the pressure was near 2.5 kb. Decrepitation halos, formed by pressure release after fluid inclusion trapping (Vityk and Bodnar 1995), occur in at least one sample from the outer zone of the pegmatite, and indicate trapping at high pressure.

A geological constraint also limits the maximum pressure. The vein-like morphology of the Morefield pegmatite, which cuts across pre-existing metamorphic foliations, is consistent with injection into brittle crust. Depending on the paleo-geothermal gradient, brittle conditions would be expected only within the upper 10 km of the crust, limiting the maximum pressure of pegmatite formation to approximately <3 kb.

When combined with the age estimates, our data suggest that cooling of the pegmatite occurred during uplift and decompression. The $^{40}Ar/^{39}Ar$ ages of the enclosing gneiss (280–260 Ma; Durrant et al. 1980) indicate when hornblende and biotite cooled through their blocking temperatures. These ages overlap the Rb-Sr ages of the pegmatite and suggest that uplift was contemporaneous with or, in part, preceded emplacement and cooling of the pegmatite. The pegmatite ages probably reflect closure of the Rb-Sr system as hydrothermal circulation through the pegmatite waned.

Sources of fluids

We interpret the multiple, apparently discrete pulses of fluids in individual microfractures as "snapshots" of the evolution of the fluid during cooling of the pegmatite. With sufficient sampling, a continuum of homogenization temperatures and salinities might be documented. The data on Figure 5, however, show no convincing evidence of a continuous cooling path, but show three apparently distinct fluid populations: One with Th >290 °C and moderate salinity; a second with Th between 150 and 230 °C and variable but higher salinity; and a third with low Th and low salinity. The fluid inclusions that plot between these populations (9 out of 150) could be those in which leakage or necking was not detected, and for which the data are therefore unreliable. The third population dominates the host gneiss sample, and thus it probably is derived from meteoric waters circulating around and through the pegmatite during cooling. Though the temperature of this fluid is similar to that of the late stage alumino-fluoride and phosphate mineral assemblages (Moore 1982), it lacks the high solute content that would be expected in the source fluids of that assemblage. The high temperature population is best interpreted as representing fluids evolved from the pegmatite itself, inasmuch as some of these inclusions occur in beryl and topaz, and the beryl sample contains no other types.

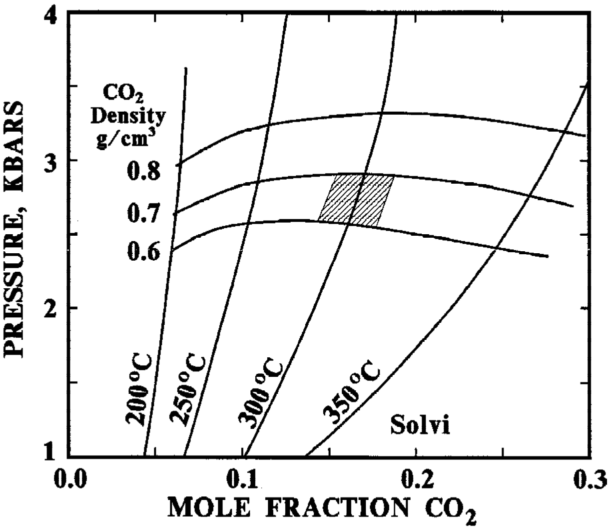

FIGURE 6. *P-X* diagram of the H_2O-rich region of the H_2O-CO_2-NaCl system (Brown and Lamb 1989). The shaded region represents probable conditions of trapping of mixed fluids at Morefield.

The origin of the higher salinity population is problematic. It cannot be derived from the high-temperature population without some mechanism for increasing fluid salinity. Phase separation could increase salinity in the H_2O-rich phase, but there is no evidence for formation of a vapor phase. Immiscibility between H_2O- and CO_2-rich fluids could increase the salinity of the H_2O fluids incrementally, possibly explaining an increase from 4 to 6 wt% NaCl (eq.), but probably not by a factor of two. Inclusions that contain solids probably have higher salinities but their relation to inclusions with 9 to 13 wt% NaCl (eq.) is unclear.

The absence of significant inclusion populations between the three groups in Figure 5 suggests that mixing between these fluid types either did not occur or that our sampling has been insufficient to document mixing. Our data indicate that fluid trapping was episodic, that only post-magmatic events are recorded in the fluid inclusions, and that even that record is incomplete.

It is unlikely that the discrete inclusion populations are an artifact related to intrusion of Mesozoic diabase dikes. The dikes are relatively thin (≤2 m) and consequently have little thermal mass: Their aureoles could not affect the pegmatite beyond about 2 m from their contacts. Though fracturing increased within 0.5 m of the dikes, no evidence exists of a thermal aureole. Chilled margins, if present, are inconspicuous. No samples were taken within 3 m of any of the dikes. The diabase is virtually anhydrous, and could not have acted as a significant fluid source. Because of their small thermal mass, the dikes could generate only a small volume of fluid by dehydration of the enclosing gneisses, and the trapping of this fluid within the pegmatite is unlikely.

Fluid inclusions do not link the Morefield pegmatite to a granitic source, but clearly exclude a genetic relation between the pegmatite and the enclosing gneiss. Most fluid inclusions in the host rock homogenize at relatively low temperature, are H_2O-rich, and have salinities <2 wt% NaCl (eq.); by comparison, the pegmatite contains higher-temperature inclusions with much more variable compositions.

Comparison with other pegmatites

Fluid inclusions in the Morefield pegmatite are less varied and reflect, in general, simpler fluid chemistry than those in other pegmatites. For example, inclusions from tourmaline-bearing pegmatites in California (Williams and Taylor 1996) contain abundant solids, but CO_2 is below levels detectable by microthermometry. Salinity and homogenization temperatures are similar to those of the Morefield inclusions, however. The pegmatite at Tanco, Manitoba (Thomas and Spooner 1988a, 1988b, 1992; Thomas et al. 1988; London 1985, 1986), which is mineralogically more complex than Morefield, has a greater range of methane content in the CO_2 phase, greater variation in CO_2 density, and higher salinity in the aqueous phase. The Harding pegmatite, New Mexico (Cook 1979), contains inclusions with higher CO_2 density and higher salinity than Morefield. At both Tanco and Harding, the greater compositional range of the fluids in part reflects preservation, in the inclusions, of more of their petrogenetic history. In these pegmatites, Li-bearing minerals provide important independent constraints on the conditions of genesis, but this support is lacking for interpretation of the fluid history of the Amelia County pegmatites.

At Morefield, as at many other pegmatites, there are abundant inclusions containing mixed CO_2-H_2O fluids with homogenization temperatures near 300 °C and density near 0.65 g/cm^3. These common features suggest similar conditions of fluid evolution; differences in observations might arise because trapping of fluids occurred at different stages in the evolution and cooling of the pegmatites. The persistent presence and elevated concentration of CO_2 in fluids of complex granitic pegmatites demonstrates that CO_2 plays a fundamental role in their genesis.

ACKNOWLEDGMENTS

This study constitutes part of the MS thesis of the senior author and was supported by research funds from the Geological Sciences Program at ODU. We acknowledge the advice and help of R.J. Bodnar. The late William D. Baltzley, former owner of Morefield, gave freely of his time in assisting with sampling of the pegmatite.

REFERENCES CITED

Bodnar, R.J. (1993) Revised equation and table for determining the freezing point depression of H_2O-NaCl solutions. Geochimica et Cosmochimica Acta, 57, 683–684.

Brown, P.E. (1989) FLINCOR: A microcomputer program for the reduction and investigation of fluid inclusion data. American Mineralogist, 74, 1390–1393.

Brown, P.E. and Lamb, W.M. (1989) P-V-T properties of fluids in the system $H_2O \pm CO_2 \pm$NaCl: New graphical presentations and implications for fluid inclusion studies. Geochimica et Cosmochimica Acta, 53, 1209–1221.

Brown, W.R. (1962) Mica and Feldspar Deposits of Virginia. Virginia Division of Mineral Resources, Mineral Resources Report 3, Charlottesville, 195 p.

Cook, C.W. (1979) Fluid inclusions and etrogenesis of the Harding Pegmatite, Taos County, New Mexico: uplublished MS thesis, University of New Mexico, Albuquerque, 143 p.

Darling, R.S. (1991) An extended equation to calculate NaCl contents from final clathrate melting temperatures in H_2O-CO_2-NaCl fluid inclusions: Implications for P-T isochore location. Geochimica et Cosmochimica Acta, 55, 3869–3871.

Deuser, W.G. and Herzog, L.F. (1962) Rubidium-strontium age determination of muscovites and biotites from pegmatites of the Blue Ridge and Piedmont. Journal of Geophysical Research, 67, 1997–2004.

Dietrich, R.V. (1990) Minerals of Virginia. Virginia Division of Mineral Resources, Charlottesville, 474 p.

Dunning, G.R. and Hodych, J.P. (1990) U/Pb zircon and baddeleyite ages for the Palisades and Gettysburg sills of the northeastern United States: Implications for the age of the Triassic/Jurassic boundary. Geology, 18, 795–798.

Durrant, J.M., Sutter, J.F., and Glover, L. III (1980) Evidence for an Alleghanian (Hercynian?) metamorphic event in the Piedmont province near Richmond, Virginia. Geological Society of America Abstracts with Programs, 12, 176.

Farrar, S.S. (1984) The Goochland granulite terrane: Remobilized Grenville basement in the eastern Virginia Piedmont. In M.J. Bartholomew, Ed., The Grenville Event in the Appalachians and Related Topics, Geological Society of America Special Paper 194, 215–227.

Foord, E.E., London, D., Kampf, A.R., Shigley, J.E., and Snee, L.W. (1991) Gem-bearing pegmatites of San Diego County, California. In M.J. Walawender and B.B. Hanan, Eds., Geological Excursions in Southern California and Mexico, p. 128–146. Geological Society of America Guidebook, Boulder, Colorado.

Frantz, J.D., Popp, R.K., and Hoering, T.C. (1992) The compositional limits of fluid immiscibility in the system H_2O-NaCl-CO_2 as determined with the use of synthetic fluid inclusions in conjunction with mass spectrometry. Chemical Geology, 98, 237–255.

Fullagar, P.D. (1971) Age and origin of plutonic intrusions in the Piedmont of the southeastern Appalachians. Geological Society of America Bulletin, 82, 2845–2862.

Fullagar, P.D. and Butler, J.R. (1979) 325 to 265 m.y. old granitic plutons in the Piedmont of the Southeastern Appalachians. American Journal of Science, 279, 161–185.

Geehan, R.W. (1953) Morefield pegmatite mine, Amelia County, Virginia. U.S. Bureau of Mines, Report of Investigations 5001, 41 p.

Glass, J.J. (1935) The pegmatite minerals from near Amelia, Virginia. American Mineralogist, 20, 741–768.

Glover, L., III, Mose, D.G., Costain, J.K., Poland, F.B., and Reilly, J.M. (1982) Grenville basement in the eastern Piedmont of Virginia: A progress report. Geological Society of America Abstracts with Programs, 14, 20.

Goldberg, S.A., Trupe, C.H., and Adams, M.G. (1992) Pressure-temperature-time constraints for a segment of the Spruce Pine thrust sheet, North Carolina Blue Ridge. Geological Society of America Abstracts with Programs, 24, 17.

Jahns, R.H., Griffitts, W.R., and Heinrich, E.W. (1952) Mica Deposits of the Southeastern Piedmont, Part 1. General Features. U.S. Geological Survey, Professional Paper 248-A, 102 p.

Kearns, L.E. (1992a) Pyromorphite from the Morefield mine, Amelia County, Virginia. Virginia Minerals, 38, 14.

——— (1992b) Prosopite from the Morefield mine, Amelia County, Virginia. Virginia Minerals, 38, 14–15.

——— (1993a) Alumino-fluoride minerals from the Morefield mine. Virginia Minerals, 39:15.

——— (1993b) Minerals of the Morefield pegmatite, Amelia County, Virginia. Rocks & Minerals, 68, 232–242.

Kish, S.A. (1977) Geochronology of plutonic activity in the Inner Piedmont and Kings Mountain Belt in North Carolina. In E.R. Burt, Ed., Field Guides for the Geological Society of America Southeastern Section Meeting, p. 144–149, North Carolina Department of Natural and Economic Resources, Winston-Salem, N.C.

Laughlin, A.W. (1966) Excess radiogenic argon in minerals from the Amelia, Virginia, pegmatites. American Geophysical Union Transactions, 47,197–198.

——— (1968) A geochronological-geochemical study of the Rutherford and Morefield pegmatites, Amelia, Virginia. American Geophysical Union Transactions, 49, 761.

——— (1969) Excess radiogenic argon in pegmatite minerals. Journal of Geophysical Research, 74, 6684–6690.

Lemke, R.W., Jahns, R.H., and Griffitts, W.R. (1952) Mica Deposits of the Southeastern Piedmont, Part 2. Amelia District, Virginia. U.S. Geological Survey, Professional Paper 248–B, 139 p.

London, D. (1985) Origin and significance of inclusions in quartz: A cautionary example from the Tanco pegmatite, Manitoba. Economic Geology, 80, 1988–1995.

——— (1986) Magmatic-hydrothermal transition in the Tanco rare-element pegmatite: Evidence from fluid inclusions and phase-equilibrium experiments. American Mineralogist, 71, 376-395.

Mitchell, R.S. and McGavock, E.H. (1960) Apatite from the Morefield pegmatite, Amelia County, Virginia. Rocks & Minerals, 35, 553–554.

Moore, P.B. (1982) Pegmatite minerals of P(V) and B(III). In P. Černý, Ed., Short Course in Granitic Pegmatites in Science and Industry. Mineralogical Association of Canada, Short Course Handbook No. 8, p. 267–291.

Rankin, D.W., Drake, A.A., Jr., Glover, L., III, Goldsmith, R., Hall, L.M., Murray, D.P., Ratcliffe, N.M., Read, J.F., Secor, D.T., Jr., and Stanley, R.S. (1989) Preorogenic terranes. In R.D. Hatcher Jr., W.A. Thomas, and G.W. Viele, Eds., The Appalachian-Ouachita Orogen in the United States, v. F-2, p. 7–100. Geological Society of America, Boulder, Colorado.

Rosso, K.M and Bodnar, R.J. (1995) Microthermometric and Raman spectroscopic detection limits of CO_2 in fluid inclusions and the Raman spectroscopic characterization of CO_2. Geochimica et Cosmochimica Acta, 59, 3961–3975.

Roedder, E. (1984) Fluid Inclusions. Mineralogical Society of America Reviews in Mineralogy, 12, 644 p.

Sinkankas, J. (1968) Classic mineral occurrences: Geology and mineralogy of the Rutherford pegmatites, Amelia, Virginia. American Mineralogist, 53, 373–405.

Smerekanicz, J.R., Dudás, F.Ö., and Baltzley, W.D. (1991) Strengite, a new mineral from the Morefield pegmatite mine, Amelia County, Virginia. Virginia Minerals, 37, 31–32.

Sterner, S.M. and Bodnar, R.J. (1991) Synthetic fluid inclusions. X: Experimental determination of P-V-T-X properties in the CO_2-H_2O system to 6 kb and 700 °C. American Journal of Science, 291, 1–54.

Sweet, P.C. and Penick, D.A., Jr. (1986) Morefield pegmatite mine reopens—Virginia's only active underground gem mine. Virginia Minerals, 32, 13–18.

Thomas, A.V. and Spooner, E.T.C. (1988a) Fluid inclusions in the system H_2O-CH_4-NaCl-CO_2 from metasomatic tourmaline within the border unit of the Tanco zoned granitic pegmatite, S.E. Manitoba. Geochimica et Cosmochimica Acta, 52, 1065–1075.

——— (1988b) Occurrence, petrology and fluid inclusion characteristics of tantalum mineralization in the Tanco granitic pegmatite, southeastern Manitoba. In R.P. Taylor and D.F. Strong, Eds., Recent Advances in the Geology of Granite-Related Mineral Deposits, Special Volume 39, 170–207. Canadian Institute of Mining and Metallurgy, Montreal.

——— (1992) The volatile geochemistry of magmatic H_2O-CO_2 fluid inclusions from the Tanco zoned granitic pegmatite, southeastern Manitoba, Canada. Geochimica et Cosmochimica Acta, 56, 49–65.

Thomas, A.V., Bray, C.J., and Spooner, E.T.C. (1988) A discussion of the Jahns-Burnham proposal for the formation of zoned granitic pegmatites using solid-liquid-vapor inclusions from the Tanco pegmatite, S.E. Manitoba. Transactions of the Royal Society of Edinburgh, 79, 299–315.

Vityk, M.O. and Bodnar, R.J. (1995) Textural evolution of synthetic fluid inclusions in quartz during reequilibration, with applications to tectonic reconstruction. Contributions to Mineralogy and Petrology, 121, 309–323.

Weis, P.L. (1953) Fluid inclusions in minerals from zoned pegmatites in the Black Hills, South Dakota. American Mineralogist, 38, 671–697.

Williams, A.E. and Taylor, M.C. (1996) Mass spectrometric identification of boric acid in fluid inclusions in pegmatite minerals. Geochimica et Cosmochimica Acta, 60, 3435–3443.

Wright, J.E., Sinha, A.K., and Glover, L., III (1975) Age of zircons from the Petersburg Granite, Virginia; with comments on belts of plutons within the Piedmont. American Journal of Science, 275, 848–856.

Zhang, Y. and Frantz, J.D. (1987) Determination of the homogenization temperatures and densities of supercritical fluids in the system NaCl-KCl-$CaCl_2$-H_2O using synthetic fluid inclusions. Chemical Geology, 64, 335–350.

MANUSCRIPT RECEIVED AUGUST 20, 1998
MANUSCRIPT ACCEPTED NOVEMBER 27, 1998
PAPER HANDLED BY DAVID LONDON